ACS OMEGA

http://pubs.acs.org/journal/acsodf

Article

Renewable and Tough Poly(L-lactic acid)/Polyurethane Blends Prepared by Dynamic Vulcanization

Seif Eddine Fenni, Francesca Bertella, Orietta Monticelli, Alejandro J. Müller, Nacerddine Hadadoui,* and Dario Cavallo*

Cite This: *ACS Omega* 2020, 5, 26421−26430

Read Online

ACCESS | Metrics & More | Article Recommendations

ABSTRACT: Melt blending of homopolymers is an effective way to achieve an attractive combination of polymer properties. Dynamic vulcanization of fatty-acid-based polyester polyol with glycerol and poly(L-lactic acid) (PLLA) in the presence of hexamethylene diisocyanate (HDI) was performed with the aim of toughening PLLA. The dynamic vulcanization in an internal mixer led to the formation of a PLLA/PU biobased blend. Melt torque, Fourier transform infrared (FTIR), and gel fraction analysis demonstrated the successful formation of cross-linked polyurethane (PU) inside the PLLA matrix. Scanning electron microscopy (SEM) analysis showed that the PLLA/PU blends exhibit a sea−island morphology. Gel fraction analysis revealed that a rubbery phase was formed inside the PLLA matrix, which was insoluble in chloroform. FTIR analysis of the insoluble part shows the appearance of an absorption band centered at 1758 cm^{-1}, related to the crystalline carbonyl vibration of the PLLA component, thus suggesting the partial involvement of PLLA chains in the cross-linking reaction. The overall content of the PU phase in the blends significantly affected the mechanical properties, thermal stability, and crystallization behavior of the materials. The overall crystallization rate of PLLA was noticeably decreased by the incorporation of PU. At the same time, polarized light optical microscopy (PLOM) analysis revealed that the presence of the PU rubbery phase inside the PLLA matrix promoted PLLA nucleation. With the formation of the PU network, the impact strength showed a remarkable increase while Young's modulus correspondingly decreased. The blends showed slightly reduced thermal stability compared to the neat PLLA.

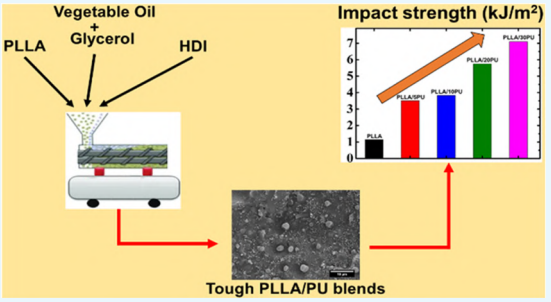

INTRODUCTION

In recent years, biodegradable polymers, especially those derived from renewable resources, have attracted increasing interest to alleviate the environmental concerns on the use of conventional petroleum-based polymers. Poly(lactic acid) (PLA) is an excellent, environmentally friendly plastic. It presents good properties, such as high rigidity and mechanical strength, high melting point, excellent biocompatibility and biodegradability, and easy processability.[1−8] However, PLA also suffers from several drawbacks, which largely restricts its widespread application. In particular, the slow crystallization kinetics, low heat distortion temperatures, and high inherent brittleness limit the applications of PLA. Therefore, significant efforts have been devoted in the last decade to enhance the properties of PLA, in particular its toughness. Several strategies have been applied to overcome brittleness such as plasticization, the addition of fillers, melt blending with flexible polymers (elastomers/rubbers), and copolymerization. Chemical modification, including grafting and reactive blending or dynamic vulcanization, was found to be an efficient approach for PLA toughening.[1,7−21]

Dynamic vulcanization and reactive blending represent a compelling way to tailor the properties and produce polymer blends with high performance. The technique involves the in situ reaction between PLA and added components during melt blending, with the formation of a cross-linked rubber phase inside the PLA matrix. Most often, the formed rubbery phase is a polyurethane (PU). PU is generally synthesized through a reaction of isocyanates (possessing more than one −NCO group) with compounds having active hydrogen functional groups, such as polyamines, polycarbonates, polyethers, and polyols (−OH). The final polyurethane product is composed of soft polymer segments (e.g., polyethers or polyols) and isocyanate-based hard/solid segments.[3,12,17,21−29]

Several works reported the dynamic vulcanization of PLA with different components, i.e., epoxidized synthetic elasto-

Received: June 11, 2020
Accepted: August 4, 2020
Published: October 8, 2020

https://dx.doi.org/10.1021/acsomega.0c02765
ACS Omega 2020, 5, 26421−26430

mers, unsaturated polymers, and natural rubber, leading to the formation of supertough PLA materials with higher mechanical characteristics. The mechanism of ductility improvement is related to two main factors, which are the chemical modification of the molecular structure and the improved compatibility between the blend component.[22,24−42]

Several examples of supertoughened PLA blends obtained by either reactive interfacial compatibilization, or dynamic vulcanization with the formation of a second component rubbery phase are reported. To prepare systems using the first strategy, several acrylate-glycidyl copolymers have been adopted, e.g., poly(ethylene-glycidyl methacrylate) (EGMA) and ethylene-*co*-acrylic ester-*co*-glycidyl methacrylate (E-AE-GMA) rubber.[43,44] Several types of rubbers vulcanized in situ within the PLA matrix have been tested, including (i) nitrile rubber cross-linked with dicumyl peroxide;[27] (ii) soybean oil vulcanized by free radical cross-linking agents;[30] (iii) zinc ionomers of the ethylene methacrylic acid copolymer (EMAA-Zn) and elastomeric ethylene-butyl acrylate-glycidyl methacrylate terpolymer (EBA-GMA);[31] and (iv) poly(glycerol succinate-*co*-maleate) (PGSMA).[41] Besides the toughening effect, in some cases, an increase in crystallization rate or nucleation density of the material was also reported.[27,34,39]

The use of isocyanate-based crosslinkers or chain extenders enables us to obtain both the formation of a dynamically vulcanized rubber phase, when reactive oligomers with low T_g are added to PLA, and the simultaneous interfacial compatibilization of the resulting blend, thanks to the reaction with the terminal hydroxyl groups of the PLA chains. Different "soft" building blocks have been used to form the polyurethane in situ, both oil-based, such as poly(ethylene glycol),[35] polyester polyol,[42] and polyurethane elastomer prepolymers;[34] or biorenewable, e.g., based on castor oil.[32,33,38,39] Largely enhanced ductility and impact resistance were reported for PLA-based blends, in addition to faster cold crystallization in most cases. Excellent compatibility of the formed rubber with PLA is generally expected because of the reported miscibility of poly(lactide) with some polyethers and polyesters.

The development of biobased rubbery tough materials remains an important research objective. Fatty-acid-based polymers are promising candidates for this aim. In this work, we aimed to toughen poly(L-lactic acid) (PLLA) and prepare an almost fully biobased material by dynamic vulcanization with hexamethylene diisocyanate (HDI), using PLLA, glycerol, and a polyester polyol derived from vegetable oils. The latter is produced by polymerization of fatty-acid dimers containing 36 carbon atoms and has the advantage of being commercially available. The morphology, thermal, and crystallization behavior were investigated and correlated with the measured mechanical properties.

RESULTS AND DISCUSSION

Chemical Analysis. Dynamic vulcanization was used to prepare PLLA/PU biobased blends in which the cross-linked PU was formed by the in situ polymerization of a polyester polyol oil, glycerol, and HDI. The reactive blending was performed in a Brabender internal mixer. All materials were prepared under the same conditions, including neat PLLA, for comparison purposes.

Interfacial compatibilization between the PLLA matrix and the PU phase can, in principle, take place, thanks to the reaction of the terminal hydroxyl groups of PLLA with the −NCO groups of HDI. Figure 1 reports the measured melt

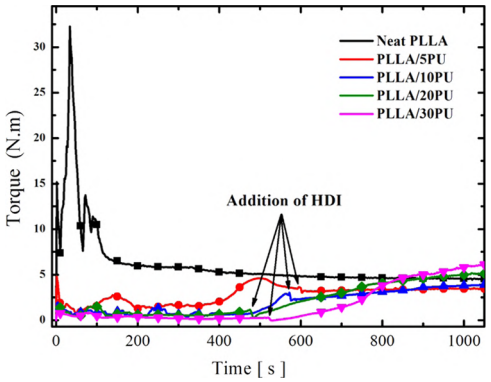

Figure 1. Torque versus time curves during the dynamic vulcanization of the different systems.

torque versus time during the dynamic vulcanization process. As judged from the instrumental response, dynamic vulcanization displays two steps. The first step is related to the melting of PLLA pellets, and it is characterized by a sharp peak in the measured torque, which decreases gradually with mixing time because of both the melting of PLLA pellets and the lubrication/plasticization effect of polyol and glycerol.[35,39] The second step starts with the addition of HDI: the torque increases gradually to an almost stable plateau because the viscosity of the system increases during the vulcanization reaction. The time at which the torque remains approximately constant indicates the end of the cross-linking process. It is worth noting that the measured torque decreases slightly when HDI is added. We hypothesize that this might be related to some extent of chain scission due to the high reactivity of the isocyanate.

To confirm the presence of a cross-linked PU network inside the PLLA matrix, we isolated a cross-linked fraction from the samples by prolonged extraction with chloroform and carried out further analysis. Figure 2 shows the weight percentage of

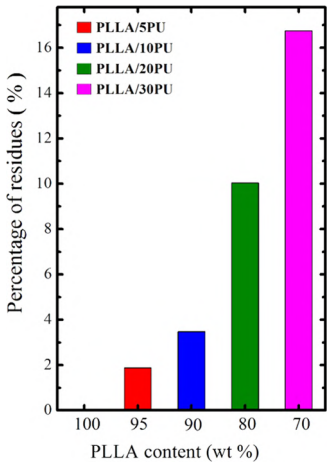

Figure 2. Percentage of the insoluble fraction (after Soxhlet extraction with chloroform) in the different PLLA/PU blends.

insoluble residues of the different PLLA/PU blends. The gel fraction increases gradually with the increase of the polyol content. However, in all cases, the vulcanized part weight was lower than the total content of the added reactive mixture (polyester polyols oil, glycerol, and HDI). This difference likely indicates that only a part of the polyol chains is

https://dx.doi.org/10.1021/acsomega.0c02765
ACS Omega 2020, 5, 26421−26430

effectively cross-linked, notwithstanding the stoichiometric ratios between isocyanate and hydroxyl groups. On the other hand, the presence of a non-negligible insoluble fraction confirms that the aim of producing a PLLA/rubber blend in situ has been achieved.

Fourier transform infrared (FTIR) was performed to confirm the occurrence of the reaction. The results related to the different as-prepared PLLA/PU blends and the insoluble fractions are reported in Figures 3 and4, respectively. All of the

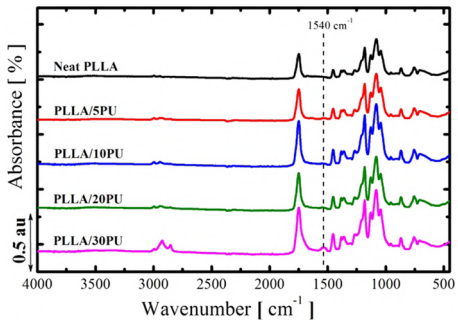

Figure 3. FTIR spectra of the different PLLA/PU blends.

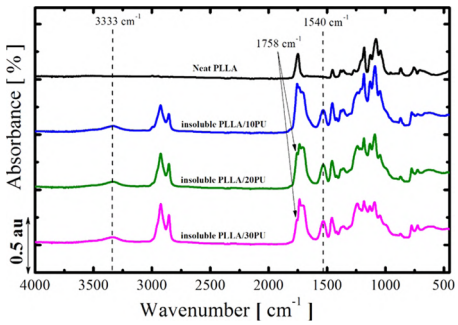

Figure 4. FTIR spectra of the neat PLLA and the insoluble fractions of different PLLA/PU blends.

characteristic absorption peaks of neat PLLA were also observed in the PLLA/PU blends spectra. Moreover, distinct absorption bands are present in the PLLA/PU samples. In particular, the peak at 1540 cm^{-1}, which characterizes the urethane group, is clearly evidenced and increases with the polyol concentration. Accordingly, no trace of the isocyanate group peak of HDI (2270 cm^{-1}) could be detected in the reacted samples.

Figure 4 shows the spectra of the neat PLLA and the insoluble fraction of PLLA/10PU, PLLA/20PU, and PLLA/30PU blends. The bands at 1540 and 3333 cm^{-1}, which are related to the urethane groups, are distinctly evident in the vulcanized fractions.[4,34] Figure 4 also reveals an absorption band centered at 1758 cm^{-1} in the spectra of insoluble fractions. This peak is related to the carbonyl group vibration of PLLA unit in the crystalline cell[5,38] and suggests the occurrence of the reaction between PLLA chains ends and HDI, to a certain extent. The obtained FTIR results confirm the successful dynamic vulcanization (of polyester polyol oil, glycerol, and HDI). They indicate the occurrence of a possible interfacial compatibilization between PLLA and PU through the formation of a chemical bond between the phases. This chemical modification will strongly affect the morphology, mechanical properties, and thermal and crystallization behavior of the final blends, as it will be shown hereafter.

Scanning Electron Microscopy (SEM). In Figure 5, some selected SEM micrographs of the cryofractured surfaces of the neat PLLA and PLLA/PU blends with different PU contents are presented. The neat PLLA showed a typical brittle fracture characterized by a smooth surface appearance. On the other hand, all of the PLLA/PU vulcanized blends exhibit a rough surface featuring a phase-separated morphology with some evidence of deformed areas. Cryofractured surfaces of PLLA/5PU, display clear cavities due to the detachment of the PU dispersed phase. This suggests a low interfacial adhesion between PLLA and PU for this blend composition. For the PU content higher than 5 wt %, the dispersed PU phases in the PLLA matrix possess an irregular shape. Good adhesion is apparent in these systems since no gaps were observed. This indicates the efficiency of the interfacial compatibilization between the two phases as a consequence of the dynamic vulcanization process. The obtained results are in agreement with the chemical changes presented in Figures 2 and 4.

On the other hand, the size of the dispersed PU phase was found to increase with the PU content, going from around 0.5−1 μm droplets in the PLLA/5PU to domains of the order of 5 μm in the PLLA/30PU blend. The increase in the PU domain size with the increase of the PU content could result from the coalescence of the PU phase, induced by its immiscibility with the PLLA matrix.

Polarized Light Optical Microscopy (PLOM). PLOM was used to study the spherulitic morphology and the superstructural growth rate of the PLLA phase within the different blends. Figure 6 shows examples of PLOM micrographs obtained for the different samples after 10 min of isothermal crystallization at 140 °C. The neat PLLA (Figure 6a) showed regular spherulites with large diameters. The regularity and perfection of the PLLA spherulites in the PLLA/PU blends decreased with the increase of the PU content, as small PU domains in the form of particlelike inclusions can be observed within the spherulite structure. In particular, at the highest content of PU, the characteristic radial fibrillar structure of the spherulite is not distinguishable anymore. The decreased PLLA spherulites regularity and texture perfection could be attributed to the interfibrillar segregation of the soft PU domains and polyols (the polyester polyol and glycerol). In fact, the micrometer-sized cross-linked polyol phase cannot be easily moved along with the growth front of the PLLA spherulites; hence, it will be engulfed inside the PLLA spherulites and thus strongly affect the lamellar arrangement. Similar results have been reported in the literature for PLLA crystallizing from an immiscible blend showing a certain interaction with the matrix.[45] Another reason that could affect the PLLA spherulites regularity is the lowered PLLA chain mobility due of the reaction with PU after dynamic vulcanization.

Besides the morphology, the nucleation density of PLLA was affected by the dynamic vulcanization and the presence of the PU phase. Hence, the number of PLLA nuclei increase significantly with the increase of PU content, as shown from an enlarged view (Figure 7). The increase in the PLLA nuclei concentration could be due to (i) some transfer of nucleating impurities from the different additives to the PLLA matrix and (ii) an interface-induced nucleation mechanism due to PLLA/PU phase separation, perhaps ascribed to local order due to the interactions between PLLA and PU.[46−49]

Results of the PLLA spherulite growth rates as a function of the chosen crystallization temperature in the studied systems are shown in Figure 8. Overall, the effect of dynamic

https://dx.doi.org/10.1021/acsomega.0c02765
ACS Omega 2020, 5, 26421−26430

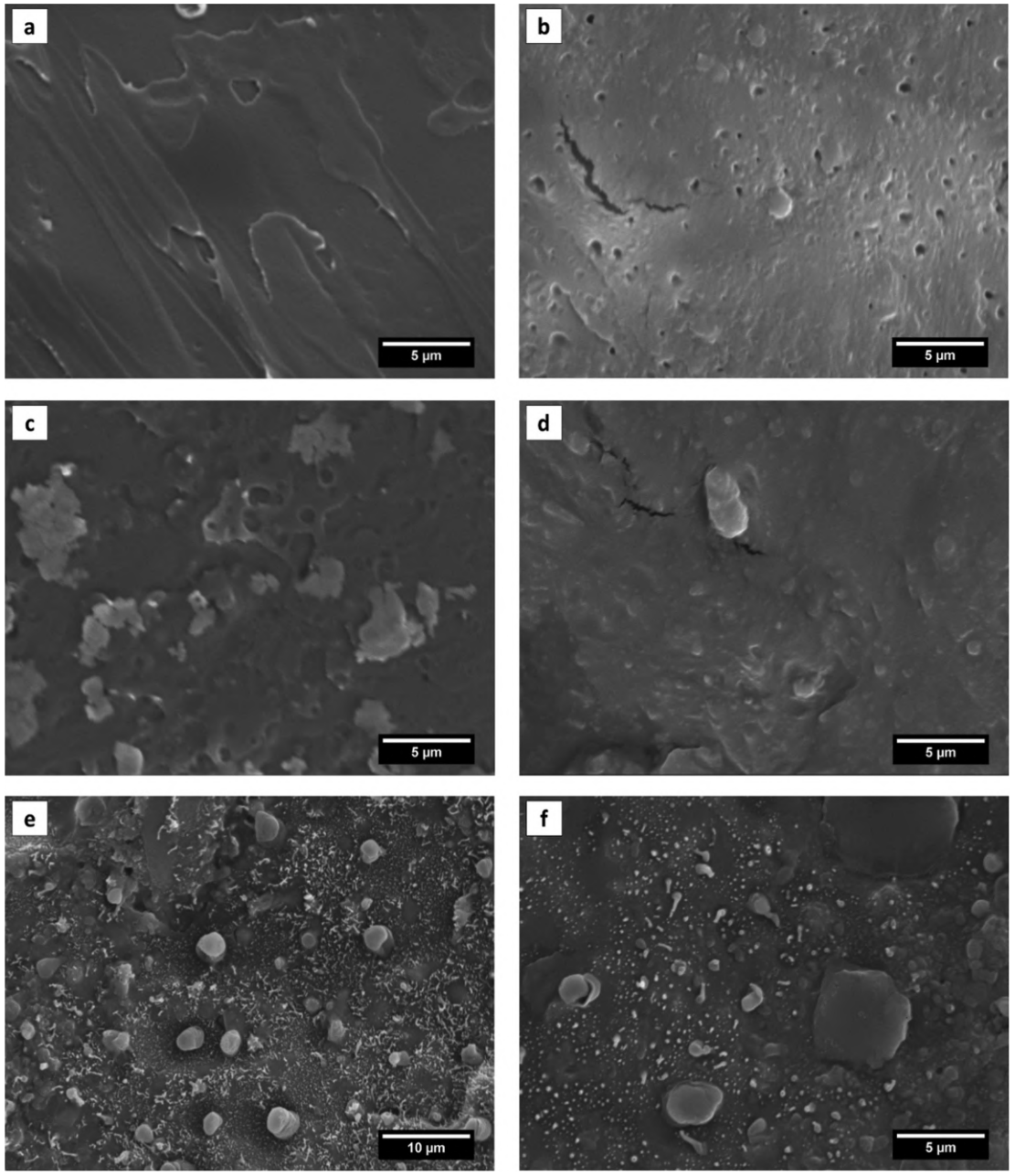

Figure 5. SEM images of different PLLA/PU blends with different concentrations of PU phase: (a) neat PLLA, (b) PLLA/5PU, (c) PLLA/10PU, (d) PLLA/20PU, and (e, f) PLLA/30PU.

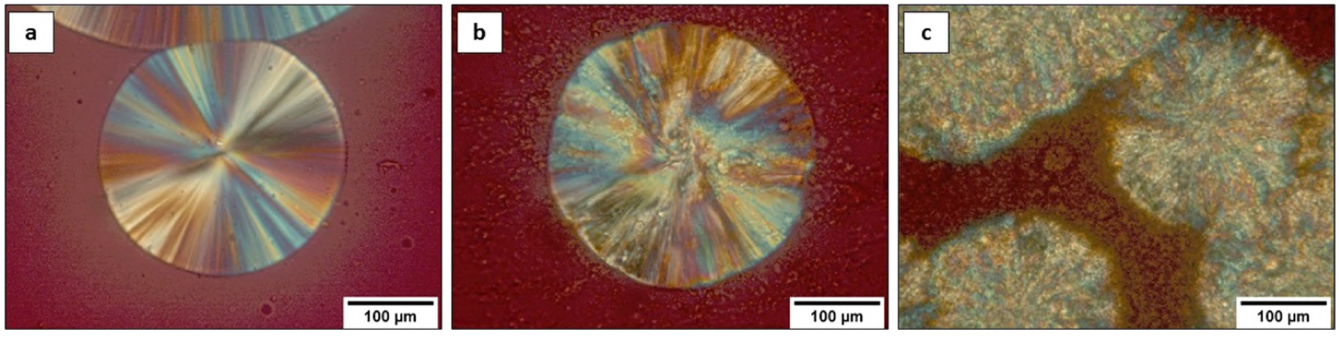

Figure 6. Polarized optical microscopy (POM) micrographs at a crystallization temperature of 140 °C for neat PLLA (a), PLLA/10PU (b), and PLLA/30PU (c).

https://dx.doi.org/10.1021/acsomega.0c02765
ACS Omega 2020, 5, 26421−26430

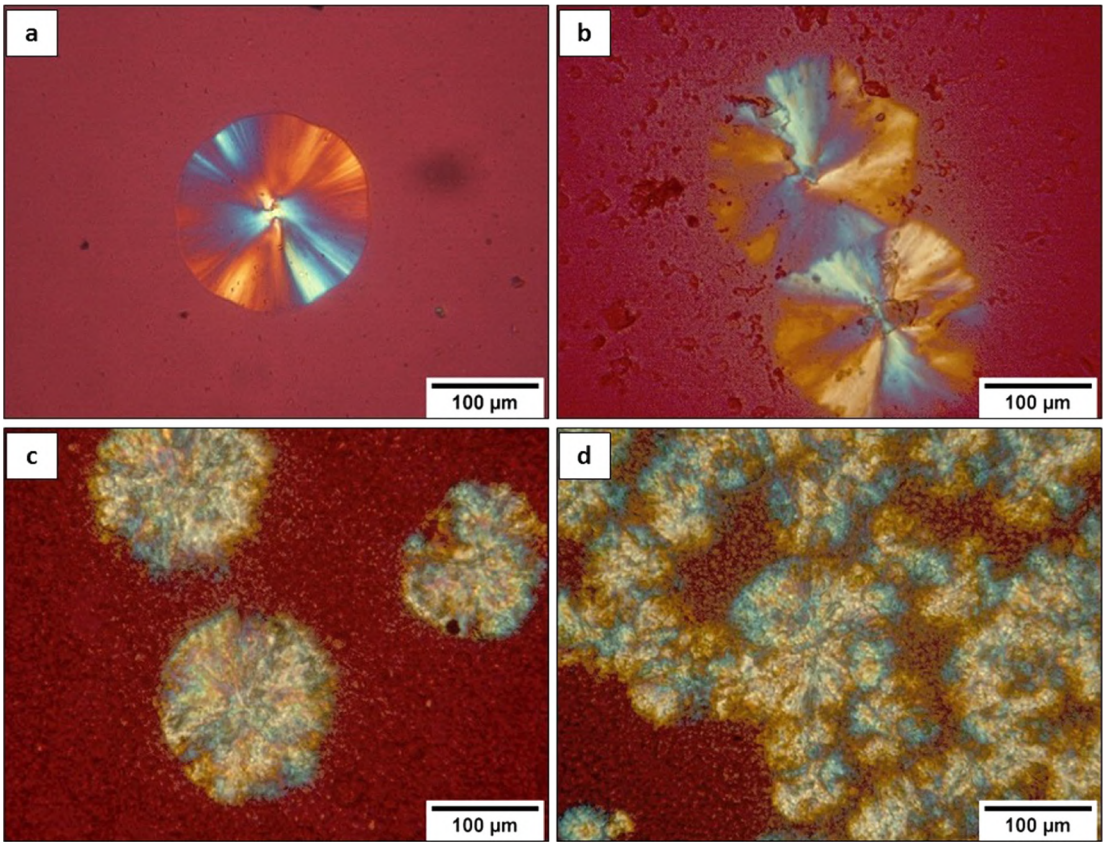

Figure 7. POM micrographs of the PLLA/PU blends after 10 min at 138 °C: (a) neat PLLA, (b) PLLA/5PU, (c) PLLA/20PU, and (d) PLLA/30PU.

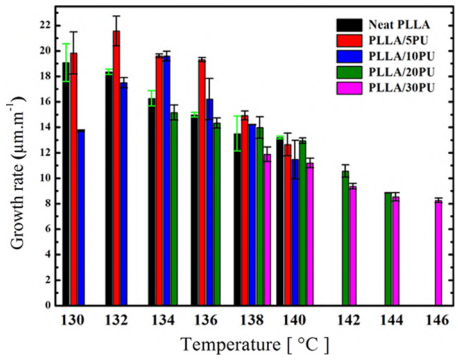

Figure 8. Growth rate of PLLA spherulites for neat PLLA and different PLLA/PU blends.

vulcanization on the growth rate is not large. This is consistent with the phase-separated blend morphology. However, some small variations could be appreciated. In particular, we note that the PLLA spherulitic growth rate of PLLA/5PU and PLLA/10PU was slightly higher than that of the neat PLLA, which is tentatively explained by a decrease in the molecular weight, due to chain scission caused by HDI and thermal degradation. Indeed, a lower molecular weight of these blends with respect to the neat PLLA could also be inferred by the lower torque value at the end of the vulcanization (Figure 1). A lower chain length leads to faster spherulitic growth.[50] For PU contents higher than 10 wt %, the PLLA growth rate is instead slightly decreased, in comparison with the other samples. Possibly, this depression is related to the extent of chemical bonding between PLLA and PU phase, which hinders the PLLA chain mobility, or the disturbance brought by the PU particles and different additives at the growth front since PU must be segregated at the interfibrillar level. This will lower the concentration of PLLA segments at the growing front and reduce the spherulitic growth rate. Due to the increased nucleation density with PU content, the minimum probed isothermal crystallization temperature, where we could clearly follow the growth rate, increased accordingly. Hence, for the neat PLLA, we were able to measure the growth rate starting from T_c of 130 °C while the minimum applied T_c was 138 °C for the PLLA/30PU blend.

Crystallization Behavior of PLLA/PU Blends by Differential Scanning Calorimetry (DSC). DSC was employed to study the thermal transitions of the neat PLLA and PLLA/PU blends. The different temperatures and enthalpies of the thermal events recorded during nonisothermal crystallization and melting at a scan rate of 10 °C/min are summarized in Table 1. At the same time, Figure 9 shows the respective DSC cooling and heating scans.

The neat PLLA crystallizes on cooling at around 103 °C, and the crystallization process is completed during the heating scan via a small cold crystallization exotherm at around 92 °C (see Figure 9a). Its endothermic melting peak was observed at 175 °C, and just before melting the PLLA crystals, a slight exothermic event is observed, tentatively attributed to the reorganization of a disordered modification into the more stable α-form.[51,52] For PLLA/PU blends with different PU contents, the DSC cooling scans show that the PLLA phase exhibits a crystallization exotherm peaked at around 106 °C for all of the samples, and the vitrification of the PLLA phase is also observed during cooling at around 63 °C, differently from

https://dx.doi.org/10.1021/acsomega.0c02765
ACS Omega 2020, 5, 26421−26430

Table 1. Transition Temperatures and Enthalpies of PLLA Phase during the Nonisothermal Scans of the Different PLLA/PU Blends at a Cooling/Heating Rate of 10 °C/min[a34]

PLLA (wt %)	T_{cc} (°C)	ΔH_{cc} (J/g)	T_c (°C)	ΔH_c (J/g)	T_m (°C)	ΔH_m (J/g)	X_c (%)
100	92.3	−0.9	102.9	−20.7	174.8	31.8	33
95	98.7	−11.8	105.4	−5.8	172.4	27.4	17
90	100	−15.2	106.7	−3.6	173.4	29.0	15
80	99.5	−11.4	106.4	−4.2	173.1	24.1	14
70	98.5	−8.3	106.6	−4.5	173.2	22.4	15

[a] ΔH_m° of 100% crystalline PLA is 93.7 J/g.

the neat PLLA where the glass transition is undetectable due to higher crystallinity. No distinct transitions or peaks related to the PU phase could be observed. The crystallization enthalpy on cooling decreases significantly in the dynamically vulcanized samples (see Table 1), testifying the hindered crystallization in the blend.

The heating process is shown in Figure 9b. The neat PLLA displays an almost negligible cold crystallization peak at around 92 °C. At the same time, the PLLA/PU blends all exhibit a larger cold crystallization peak at about 99 °C. The cold crystallization enthalpy was affected as well and increased largely in the PLLA/PU blends (from 0.9 J/g in the neat PLLA to 8 J/g in PLLA/30PU). The crystallinity degree (X_c%) of PLLA at the end of the temperature protocol, evaluated from the measured melting enthalpy after correction for the PLLA weight fraction in the particular blend, dropped from 33% for the neat PLLA to around 15% when the vulcanized PU is added. We must deduce that a meaningful hindrance effect of the PU phase on the crystallization is present, when the process occurs at temperatures lower than those probed by PLOM experiments. In fact, a significant decrease in the growth rate was only observed for the PLLA/30PU sample in the probed temperature range (as observed by PLOM). These noticeable decreases in the crystallinity, as shown by the DSC analysis, might be due to the higher viscosity of the blends compared to that of the neat PLLA.

Thermal Stability of the PLLA/PU Blends. Thermal stability of the neat PLLA and PLLA/PU blends under nonoxidative conditions was investigated by thermogravimetric analysis (TGA). The analysis was performed in the range of 25−800 °C at a heating rate of 10 °C/min under a constant nitrogen gas flow. Figure 10 shows the TGA weight loss curves as a function of temperature. From these curves, we can identify the onset and end of the thermal decomposition, indicated by T_5 (5% of mass loss) and T_{end} (100% of mass loss), respectively.

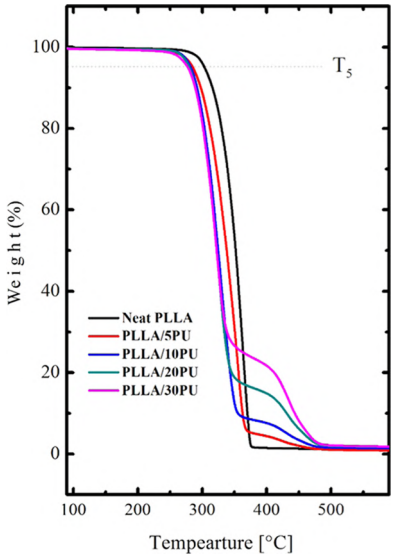

Figure 10. TGA curves of the PLLA and PLLA/PU blends.

The neat PLLA displays a single-stage decomposition process, with T_5 = 304 °C and T_{end} around 374 °C. On the other hand, all the PLLA/PU blends show a two-stage decomposition, obviously related to the presence of two chemically distinct units, the PLLA and polyol phases. In fact, the magnitude of mass loss at the different steps varies in agreement with the blend composition, i.e., the percentage of low-temperature decomposition event decreases with increasing PU fraction and vice versa for the high-temperature event. An almost quantitative relation with the nominal content of PU is found.

For what concerns the degradation temperatures, the onset of PLLA degradation shifts to lower temperature after dynamic

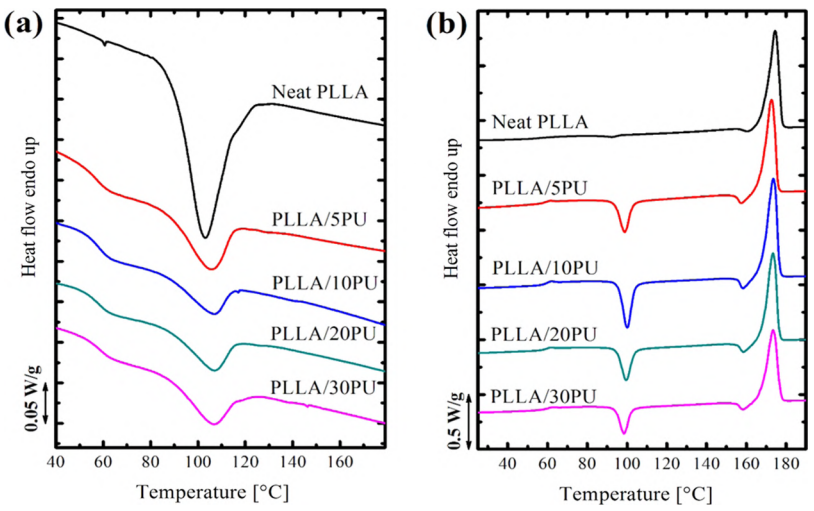

Figure 9. DSC cooling (a) and heating (b) curves recorded at a scan rate of 10 °C/min for neat PLLA and PLLA/PU blends.

https://dx.doi.org/10.1021/acsomega.0c02765
ACS Omega 2020, 5, 26421−26430

vulcanization and with the increasing PU phase content. In particular, T_5 decreased from 304 °C for the neat PLLA to around 276 °C for PLLA/30PU.

The decomposition stage with T_{end} around 336 °C observed in the blends was attributed to the urethane bonds breaking,[39] while the decomposition event ending at around 485 °C can be ascribed to the thermal degradation of the aliphatic segments of the polyester polyol.[53]

Notwithstanding the slight decrease in the temperature of initial thermal degradation, a good thermal stability of different blends was observed, since the values of the decomposition temperatures are still at least 50 °C above the commonly employed processing temperature.

Tensile and Impact Properties. Generally, the mechanical properties of interest of polymers are related to their strength and toughness. Tensile elongation at the break and the impact strength are considered as measures of material's toughness, whereas the flexural modulus and tensile strength at the break are informative of material's strength.[38,54] Figure 11 shows the

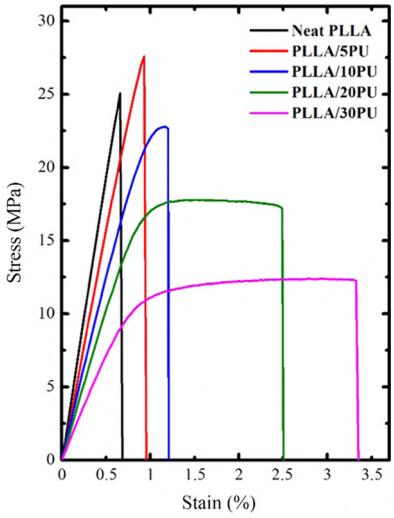

Figure 11. Tensile stress−strain curves for the neat PLLA and PLLA/PU blends.

corresponding stress−strain curves, while Figure 12a summarizes the results of the mechanical tensile test on different systems. The inclusion of vulcanized PU phase affects the system's strength and rigidity. In particular, Young's modulus

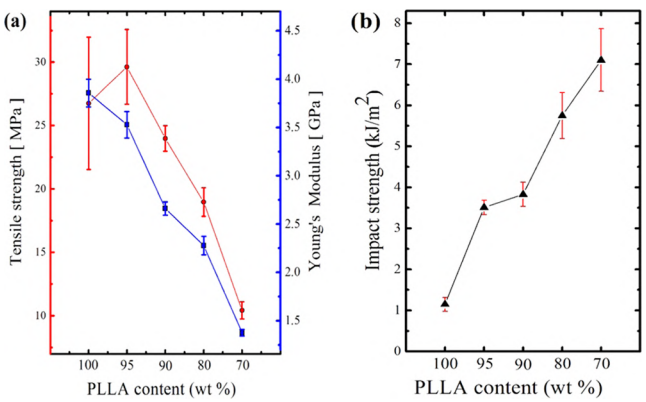

Figure 12. (a) Tensile strength and Young's modulus. (b) Impact strength of PLLA and the PLLA/PU blends.

decreases steadily to about one third its value in the neat PLLA when the PU content in the blend is 30 wt % of PU. Similarly, the stress at the break of the same blend is about 2 times lower than that of the neat PLLA. However, this softening of the material is not accompanied by a significant increase in the elongation at break, which keeps very low, below 2% strain.

As such, the modified PLLA still behaves as a brittle material upon tensile deformation. The behavior of the PLLA matrix dominates the mechanical response of the blend perhaps due to insufficient degree of molecular interactions between the two components, which leads to interfacial debonding, and the lack of any plasticization effects of the polyol segments on PLLA.

On the other hand, the Charpy impact tests revealed a reasonably good improvement in the impact strength values of the PLLA/PU blends. More specifically, the impact strength of the neat PLLA was found to be around 1 kJ/m^2, indicating the brittle nature of the material. In comparison, significant improvement of the impact strength of the PLLA/PU blends was observed; thus, the impact strength increases gradually with the PU content (see Figure 12b) up to a value of 7 kJ/m^2 for the PLLA/30PU blend (approximately 7 times that the value of the neat PLLA). It is deduced that the dispersed PU rubbery domains can partially absorb the energy released upon impact and hinder the crack growth, thus providing higher toughness to the PLLA/PU blends.[35,38,55] However, in the tensile deformation mode, the failure of the sample is still dominated by the strong tendency of the PLLA matrix to localize plastic deformation, which easily leads to the development of crazes.

Similar enhancements of the impact strength of dynamically vulcanized PLA were reported in the case of poly(L-lactic acid)/poly(butylene succinate)/dicumyl peroxide (PLLA/PBS/DCP),[3] poly(lactic acid)/thermoplastic starch (PLA/TPS),[25] poly(L-lactic acid)/nitrile-butadiene rubber (PLLA/NBR),[27] poly(lactic acid)/polyurethane elastomer prepolymer (PLA/PUEP),[34] polylactide/cross-linked polyurethane (PLA/CPU),[35] poly(lactic acid)/ethylene-methyl acrylate-glycidyl methacrylate (PLA/EMA-GMA),[36] polylactide/castor oil-based polyurethane prepolymer (PLA/COPUP),[38] and poly(lactic acid)/poly(glycerol succinate-*co*-maleate) (PLA/PGSMA).[41]

CONCLUSIONS

The present work discusses the efficiency of dynamic vulcanization reaction and the formation of a PU phase for toughening brittle PLLA. The dynamic vulcanization of PLLA, polyester polyol, glycerol, and HDI was successfully accomplished, and almost fully biobased PLLA/PU blends were obtained. An analysis of the FTIR spectra, extracted and insoluble fractions, and the evolution of torque during sample preparation demonstrated the in situ formation of a PU phase, thanks to the reaction between −NCO groups of HDI with the −OH groups of the polyester polyol, glycerol, and PLLA. The partial reaction with PLLA chain gives rise to some extent of interfacial compatibilization between PLLA and dispersed PU phase. The impact strength was significantly increased by the increase in the PU content; however, the tensile properties were not largely enhanced. For what concerns the thermal properties, DSC showed a depression in the nonisothermal crystallization rate of the blends, as compared to the neat PLLA. Thermogravimetric analysis demonstrated that all

https://dx.doi.org/10.1021/acsomega.0c02765
ACS Omega 2020, 5, 26421−26430

PLLA/PU blends were sufficiently stable at the typical processing temperatures of PLLA.

Dynamic vulcanization to enable the in situ formation of a biobased elastomeric phase is thus proposed as a promising route for the improvement of PLLA properties for potentially widening its application range.

MATERIALS AND METHODS

Materials. Poly(L-lactic acid) (PLLA) (Synterra 1010) was supplied by Synbra Technology (Etten-Leur, Netherlands). PLLA 1010 is a crystallizable grade of PLLA with an L-lactide content of about 99 wt % and an average molecular weight of 1 × 10^5 g/mol. The melting point is in the range 175−180 °C, and the glass transition temperature (T_g) is around 55−60 °C. The polymer shows a melt flow rate (MFR) of about 12 g/10 min (190 °C, 2.16 kg, ISO 1133) and a density of 1.25 g/cm^3. PLLA was dried at 60 °C overnight prior to use.

Priplast 3196 is a dimerized fatty-acid-based polyester polyol with molecular weight of 3 kg/mol. The polyol has been synthesized from C36 fatty-acid dimers derivative, in turn, obtained by dimerization of unsaturated C18 fatty acids (such as oleic, linoleic, and linolenic acids). This material was kindly supplied by Croda Factory. Glycerol (49767) with a glycerol content of 99.5%, hexamethylene diisocyanate (HDI, 52649) (≥99%), and chloroform (C2432) with a purity of 99.5% were purchased from Sigma-Aldrich and used as received. Cellulose extraction thimbles (Grade 208) were purchased from AquaLab technologies.

Sample Preparation. Dynamic vulcanization of the Priplast 3196 and glycerol in the presence of HDI inside the PLLA matrix was performed in a Plastograph Brabender internal mixer (W50 EHT, Brabender GmbH, Germany) at 200 °C using a rotor speed of 60 rpm for sufficient time (around 18 min). PLLA, polyol, and glycerol in predetermined amounts were first premixed in the Brabender at 200 °C and 60 rpm for 8 min to obtain a uniform melt. Then dynamic vulcanization of the polyol and glycerol was initiated by adding HDI under the same mixing conditions. An initial mass of around 40 g was used in each blend and a final yield of about 80−85% was obtained.

When the dynamic vulcanization occurred, the melt torque increased first and then leveled off (after approximately 10 min), which was interpreted as the end of the dynamic vulcanization process. The molar ratio of the −NCO group of HDI to the −OH group (of the polyol and glycerol) was fixed at 1:1, while the glycerol/polyol weight ratio was kept at about 10%. Five samples with the PLLA weight fraction of 100, 95, 90, 80, and 70 were prepared. The respective sample codes are reported in Table 2. For the sake of comparison, the neat PLLA was also treated under the same processing conditions in the internal mixer.

Blend Characterization. *Determination of the Cross-Linked Fraction.* Samples with a predetermined weight ($m_i \approx 1$ g) were enclosed into cellulose extraction thimbles. The extraction was performed using a Soxhlet extractor for 3 days with an excess volume of boiling chloroform. The fraction of the sample that did not dissolve in chloroform but just swelled was then weighed (m_f) after complete drying under vacuum at room temperature. The insoluble fraction must consist of the vulcanized PU and possibly PLLA chains, which reacted with PU. The cross-linked fraction was calculated according to eq 1

$$\text{cross} - \text{linked fraction}\ (\%) = (m_f/m_i) \times 100 \quad (1)$$

Table 2. Composition of the Prepared Samples (in Weight Percentage, wt %)

sample	PLLA (wt %)	priplast 3196 (wt %)	glycerol (wt %)	HDI (wt %)
neat PLLA	100	0	0	0
PLLA/5PU	95	3.42	0.38	1.2
PLLA/10PU	90	6.84	0.76	2.4
PLLA/20PU	80	13.68	1.52	4.8
PLLA/30PU	70	20.52	2.28	7.2

where m_i is the initial sample weight and m_f is the weight of the insoluble part after extraction.[34]

Fourier Transform Infrared Analysis. FTIR spectra of the PLLA/PU blends and insoluble sample fractions were recorded at room temperature using a Bruker IFS66 spectrometer equipped with an attenuated total reflectance (ATR) accessory. A total of 32 spectra with a resolution of 4 cm^{-1} were acquired for each sample in the range 500−4000 cm^{-1}.

Scanning Electron Microscopy (SEM). Different PLLA/PU blends were cryogenically fractured after 3 h of immersion in liquid nitrogen. The fracture surfaces were observed by SEM after gold coating under vacuum using a Hitachi S-2700 electron microscope. Micrographs of the most representative inner regions of the specimens are reported.

Polarized Light Optical Microscopy. PLOM was employed to determine the morphology and measure the growth rate of PLLA spherulites. Films with a thickness of around 30 μm were prepared by microtoming and by gentle compression molding between two microscope glass slides on a hot plate. The micrographs of blend films were recorded with a LEICA DC 420 camera. A METTLER FP35Hz hot stage was employed to impose the desired thermal history.

The isothermal spherulitic growth rates of the neat PLLA and the PLLA phase within the PLLA/PU blends were measured. The samples were first heated to 200 °C for 3 min to erase the previous thermal history and then cooled to the chosen crystallization temperature, at which spherulitic growth was monitored in time by suitable image acquisition.

Differential Scanning Calorimetry. DSC was performed using a DSC1 STAR^e system (Mettler-Toledo, Switzerland). The samples, with weight in the range of 3−5 mg and prepared by gentle compression molding between two glass slides, were melted at 200 °C for 3 min and then cooled to −50 °C at a rate of 10 °C/min. After cooling, the polymers were subsequently heated to 200 °C at 10 °C/min. During the DSC runs, a nitrogen flow at a rate of 20 mL/min was constantly applied. The crystallinity degree X_c (%) of the PLLA component in the different blends was calculated using the following formula

$$X_c\ (\%) = (\Delta H_m - \Delta H_{cc})/(\Delta H_m^\circ \times W_f) \quad (2)$$

where ΔH_m and ΔH_{cc} are the measured enthalpies of melting and cold crystallization for the PLLA phase in the blends, ΔH_m° is the melting enthalpy of 100% crystalline PLA (93.7 J/g), and W_f is the weight fraction of PLLA in the blend.[34]

Thermogravimetric Analysis (TGA). TGA was performed using TGA Mettler-Toledo (STAR^e system Mettler thermobalance). The temperature was increased from 25 to 800 °C

https://dx.doi.org/10.1021/acsomega.0c02765
ACS Omega 2020, 5, 26421−26430

with a heating rate of 10 °C/min under a nitrogen flow of 80 mL/min (Table 2).

Tensile Tests. The tensile properties of the PLLA/PU blends were determined with an Instron mechanical tester (Instron 5565) using a crosshead speed of 5 mm/min and dog bone specimens according to the ASTM-D638 standard. The specimens were cut from a compression molded plate, which, in turn, was prepared by compression of the blend in a "CARVER" manual press at 200 °C and 3.5 ton for 3 min, followed by continuous cooling to room temperature with tap water. The reported measured properties (Young's modulus, strength, and deformation at the break) are average values from five different specimens.

Impact Test. The impact strengths of different PLLA/PU blends were measured using a Pendulum Impact Testing Machine (Charpy Zwick 5102). The specimens of 60 mm × 10 mm × 2 mm were cut from a compression molded plate (prepared as mentioned in the tensile section) and a small notch (of around 1 mm in depth) was produced by means of a manual saw. The measured values are of significance for a relative comparison between the neat and the blended PLLA materials only, given that customized (nonstandard) sample preparation procedure and test were adopted. Five analyses were performed for each sample, and the average values are reported.

AUTHOR INFORMATION

Corresponding Authors

Nacerddine Hadadoui − *Laboratory of Physical-Chemistry of High Polymers (LPCHP), Faculty of Technology, University of Ferhat ABBAS Sétif-1, 19000 Sétif, Algeria*; Email: n_haddaoui@univ-setif.dz

Dario Cavallo − *Department of Chemistry and Industrial Chemistry, University of Genova, 16146 Genova, Italy*; orcid.org/0000-0002-3274-7067; Email: dario.cavallo@unige.it

Authors

Seif Eddine Fenni − *Department of Chemistry and Industrial Chemistry, University of Genova, 16146 Genova, Italy; Laboratory of Physical-Chemistry of High Polymers (LPCHP), Faculty of Technology, University of Ferhat ABBAS Sétif-1, 19000 Sétif, Algeria*

Francesca Bertella − *Department of Chemistry and Industrial Chemistry, University of Genova, 16146 Genova, Italy*

Orietta Monticelli − *Department of Chemistry and Industrial Chemistry, University of Genova, 16146 Genova, Italy*; orcid.org/0000-0003-4999-3069

Alejandro J. Müller − *POLYMAT and Polymer Science and Technology Department, Faculty of Chemistry, University of the Basque Country UPV/EHU, 20018 Donostia-San Sebastiá, Spain; IKERBASQUE, Basque Foundation for Science, 48013 Bilbao, Spain*; orcid.org/0000-0001-7009-7715

Complete contact information is available at: https://pubs.acs.org/10.1021/acsomega.0c02765

Notes

The authors declare no competing financial interest.

ACKNOWLEDGMENTS

This work has received funding from the European Union's Horizon 2020 research and innovation program under the Marie Sklodowska-Curie grant agreement no. 778092

REFERENCES

(1) Bhardwaj, R.; Mohanty, A. K. Modification of brittle polylactide by novel hyperbranched polymer-based nanostructures. *Biomacromolecules* **2007**, *8*, 2476−2484.

(2) Yokohara, T.; Yamaguchi, M. Structure and properties for biomass-based polyester blends of PLA and PBS. *Eur. Polym. J.* **2008**, *44*, 677−685.

(3) Wang, R.; Wang, S.; Zhang, Y.; Wan, C.; Ma, P. Toughening modification of PLLA/PBS blends via in situ compatibilization. *Polym. Eng. Sci.* **2009**, *49*, 26−33.

(4) Cai, Y.; Lv, J.; Feng, J. Spectral Characterization of Four Kinds of Biodegradable Plastics: Poly (Lactic Acid), Poly (Butylenes Adipate-Co-Terephthalate), Poly (Hydroxybutyrate-Co-Hydroxyvalerate) and Poly (Butylenes Succinate) with FTIR and Raman Spectroscopy. *J. Polym. Environ.* **2013**, *21*, 108−114.

(5) Di Lorenzo, M. L.; Rubino, P.; Cocca, M. Miscibility and properties of poly(l-lactic acid)/poly(butylene terephthalate) blends. *Eur. Polym. J.* **2013**, *49*, 3309−3317.

(6) Homklin, R.; Hongsriphan, N. Mechanical and Thermal Properties of PLA/PBS Co-continuous Blends Adding Nucleating Agent. *Energy Procedia* **2013**, *34*, 871−879.

(7) Hamad, K.; Kaseem, M.; Yang, H. W.; Deri, F.; Ko, Y. G. Properties and medical applications of polylactic acid: A review. *Express Polym. Lett.* **2015**, *9*, 435−455.

(8) Farah, S.; Anderson, D. G.; Langer, R. Physical and mechanical properties of PLA, and their functions in widespread applications — A comprehensive review. *Adv. Drug Delivery Rev.* **2016**, *107*, 367−392.

(9) Paul, D. R.; Barlow, J. W. A Brief Review of Polymer Blend Technology. In *Multiphase Polymers*; American Chemical Society, 1979; Vol. *176*, pp 315−335.

(10) Kobayashi, J.; Asahi, T.; Ichiki, M.; Oikawa, A.; Suzuki, H.; Watanabe, T.; Fukada, E.; Shikinami, Y. Structural and optical properties of poly lactic acids. *J. Appl. Phys.* **1995**, *77*, 2957−2973.

(11) Mathew, A. P.; Oksman, K.; Sain, M. Mechanical properties of biodegradable composites from poly lactic acid (PLA) and microcrystalline cellulose (MCC). *J. Appl. Polym. Sci.* **2005**, *97*, 2014−2025.

(12) Madhavan Nampoothiri, K.; Nair, N. R.; John, R. P. An overview of the recent developments in polylactide (PLA) research. *Bioresour. Technol.* **2010**, *101*, 8493−8501.

(13) Theryo, G.; Jing, F.; Pitet, L. M.; Hillmyer, M. A. Tough Polylactide Graft Copolymers. *Macromolecules* **2010**, *43*, 7394−7397.

(14) Robeson, L. Historical Perspective of Advances in the Science and Technology of Polymer Blends. *Polymers* **2014**, *6*, 1251.

(15) Tawakkal, I. S. M. A.; Cran, M. J.; Miltz, J.; Bigger, S. W. A Review of Poly(Lactic Acid)-Based Materials for Antimicrobial Packaging. *J. Food Sci.* **2014**, *79*, R1477−R1490.

(16) Kamthai, S.; Magaraphan, R. In *Thermal and Mechanical Properties of Polylactic Acid (PLA) and Bagasse Carboxymethyl Cellulose (CMCB) Composite by Adding Isosorbide Diesters*, AIP Publishing, 2015; 060006.

(17) Nagarajan, V.; Mohanty, A. K.; Misra, M. Perspective on Polylactic Acid (PLA) based Sustainable Materials for Durable Applications: Focus on Toughness and Heat Resistance. *ACS Sustainable Chem. Eng.* **2016**, *4*, 2899−2916.

(18) Ock, H. G.; Kim, D. H.; Ahn, K. H.; Lee, S. J.; Maia, J. M. Effect of organoclay as a compatibilizer in poly(lactic acid) and natural rubber blends. *Eur. Polym. J.* **2016**, *76*, 216−227.

(19) Jia, S.; Yu, D.; Zhu, Y.; Wang, Z.; Chen, L.; Fu, L. Morphology, Crystallization and Thermal Behaviors of PLA-Based Composites: Wonderful Effects of Hybrid GO/PEG via Dynamic Impregnating. *Polymers* **2017**, *9*, No. 528.

(20) Nakajima, H.; Dijkstra, P.; Loos, K. The Recent Developments in Biobased Polymers toward General and Engineering Applications: Polymers that are Upgraded from Biodegradable Polymers, Analogous to Petroleum-Derived Polymers, and Newly Developed. *Polymers* **2017**, *9*, No. 523.

(21) Wang, M.; Wu, Y.; Li, Y.-D.; Zeng, J.-B. Progress in Toughening Poly(Lactic Acid) with Renewable Polymers. *Polym. Rev.* **2017**, *57*, 557−593.

(22) Chen, G.-X.; Kim, H.-S.; Kim, E.-S.; Yoon, J.-S. Compatibilization-like effect of reactive organoclay on the poly(l-lactide)/poly(butylene succinate) blends. *Polymer* **2005**, *46*, 11829−11836.
(23) Anderson, K. S.; Schreck, K. M.; Hillmyer, M. A. Toughening Polylactide. *Polym. Rev.* **2008**, *48*, 85−108.
(24) Nerkar, M.; Ramsay, J. A.; Ramsay, B. A.; Vasileiou, A. A.; Kontopoulou, M. Improvements in the melt and solid-state properties of poly(lactic acid), poly-3-hydroxyoctanoate and their blends through reactive modification. *Polymer* **2015**, *64*, 51−61.
(25) Akrami, M.; Ghasemi, I.; Azizi, H.; Karrabi, M.; Seyedabadi, M. A new approach in compatibilization of the poly(lactic acid)/thermoplastic starch (PLA/TPS) blends. *Carbohydr. Polym.* **2016**, *144*, 254−262.
(26) Hu, X.; Li, Y.; Li, M.; Kang, H.; Zhang, L. Renewable and Supertoughened Polylactide-Based Composites: Morphology, Interfacial Compatibilization, and Toughening Mechanism. *Ind. Eng. Chem. Res.* **2016**, *55*, 9195−9204.
(27) Liu, L.; Hou, J.; Wang, L.; Zhang, J.; Duan, Y. Role of Dicumyl Peroxide on Toughening PLLA via Dynamic Vulcanization. *Ind. Eng. Chem. Res.* **2016**, *55*, 9907−9914.
(28) Ma, M.; Zheng, H.; Chen, S.; Wu, B.; He, H.; Chen, L.; Wang, X. Super-toughened poly(l-lactic acid) fabricated via reactive blending and interfacial compatibilization. *Polym. Int.* **2016**, *65*, 1187−1194.
(29) Formela, K.; Zedler, L.; Hejna, A.; Tercjak, A. Reactive extrusion of bio-based polymer blends and composites − Current trends and future developments. *Express Polym. Lett.* **2018**, *12*, 24−57.
(30) Robertson, M. L.; Chang, K.; Gramlich, W. M.; Hillmyer, M. A. Toughening of Polylactide with Polymerized Soybean Oil. *Macromolecules* **2010**, *43*, 1807−1814.
(31) Liu, H.; Song, W.; Chen, F.; Guo, L.; Zhang, J. Interaction of Microstructure and Interfacial Adhesion on Impact Performance of Polylactide (PLA) Ternary Blends. *Macromolecules* **2011**, *44*, 1513−1522.
(32) Robertson, M. L.; Paxton, J. M.; Hillmyer, M. A. Tough Blends of Polylactide and Castor Oil. *ACS Appl. Mater. Interfaces* **2011**, *3*, 3402−3410.
(33) Gurunathan, T.; Mohanty, S.; Nayak, S. K. Preparation and performance evaluation of castor oil-based polyurethane prepolymer/polylactide blends. *J. Mater. Sci.* **2014**, *49*, 8016−8030.
(34) Lu, X.; Wei, X.; Huang, J.; Yang, L.; Zhang, G.; He, G.; Wang, M.; Qu, J. Supertoughened Poly(lactic acid)/Polyurethane Blend Material by in Situ Reactive Interfacial Compatibilization via Dynamic Vulcanization. *Ind. Eng. Chem. Res.* **2014**, *53*, 17386−17393.
(35) Liu, G.-C.; He, Y.-S.; Zeng, J.-B.; Xu, Y.; Wang, Y.-Z. In situ formed crosslinked polyurethane toughened polylactide. *Polym. Chem.* **2014**, *5*, 2530−2539.
(36) Zhang, K.; Nagarajan, V.; Misra, M.; Mohanty, A. K. Supertoughened renewable PLA reactive multiphase blends system: phase morphology and performance. *ACS Appl. Mater. Interfaces* **2014**, *6*, 12436−12448.
(37) Kunduru, K. R.; Basu, A.; Haim Zada, M.; Domb, A. J. Castor Oil-Based Biodegradable Polyesters. *Biomacromolecules* **2015**, *16*, 2572−2587.
(38) Gurunathan, T.; Chung, J. S.; Nayak, S. K. Reactive Compatibilization of Biobased Polyurethane Prepolymer Toughening Polylactide Prepared by Melt Blending. *J. Polym. Environ.* **2016**, *24*, 287−297.
(39) Zhao, T.-H.; He, Y.; Li, Y.-D.; Wang, M.; Zeng, J.-B. Dynamic vulcanization of castor oil in a polylactide matrix for toughening. *RSC Adv.* **2016**, *6*, 79542−79553.
(40) Das, S.; Pandey, P.; Mohanty, S.; Nayak, S. K. Insight on Castor Oil Based Polyurethane and Nanocomposites: Recent Trends and Development. *Polym.-Plast. Technol. Eng.* **2017**, *56*, 1556−1585.
(41) Valerio, O.; Misra, M.; Mohanty, A. K. Sustainable biobased blends of poly(lactic acid) (PLA) and poly(glycerol succinate-co-maleate) (PGSMA) with balanced performance prepared by dynamic vulcanization. *RSC Adv.* **2017**, *7*, 38594−38603.
(42) Zhao, X.; Ding, Z.; Lin, Q.; Peng, S.; Fang, P. Toughening of polylactide via in situ formation of polyurethane crosslinked elastomer during reactive blending. *J. Appl. Polym. Sci.* **2017**, *134*, No. 44383.
(43) Oyama, H. T. Super-tough poly(lactic acid) materials: Reactive blending with ethylene copolymer. *Polymer* **2009**, *50*, 747−751.
(44) Dong, W.; Jiang, F.; Zhao, L.; You, J.; Cao, X.; Li, Y. PLLA Microalloys Versus PLLA Nanoalloys: Preparation, Morphologies, and Properties. *ACS Appl. Mater. Interfaces* **2012**, *4*, 3667−3675.
(45) Park, J. W.; Im, S. S. Miscibility and morphology in blends of poly(l-lactic acid) and poly(vinyl acetate-co-vinyl alcohol). *Polymer* **2003**, *44*, 4341−4354.
(46) Pan, P.; Shan, G.; Bao, Y. Enhanced Nucleation and Crystallization of Poly(l-lactic acid) by Immiscible Blending with Poly(vinylidene fluoride). *Ind. Eng. Chem. Res.* **2014**, *53*, 3148−3156.
(47) Shi, W.; Chen, F.; Zhang, Y.; Han, C. C. Viscoelastic Phase Separation and Interface Assisted Crystallization in a Highly Immiscible iPP/PMMA Blend. *ACS Macro Lett.* **2012**, *1*, 1086−1089.
(48) Yu, C.; Han, L.; Bao, J.; Shan, G.; Bao, Y.; Pan, P. Polymorphic Crystallization and Crystalline Reorganization of Poly(l-lactic acid)/Poly(d-lactic acid) Racemic Mixture Influenced by Blending with Poly(vinylidene fluoride). *J. Phys. Chem. B* **2016**, *120*, 8046−8054.
(49) Fenni, S. E.; Cavallo, D.; Müller, A. J. Nucleation and Crystallization in Bio-Based Immiscible Polyester Blends. In *Thermal Properties of Bio-Based Polymers*;Lorenzo, M. L. D.; Androsch, R., Eds.; Advances in Polymer Science; Springer International Publishing: Cham, 2019; Vol. *283*, pp 219−256.
(50) Santonja-Blasco, L.; Ribes-Greus, A.; Alamo, R. G. Comparative thermal, biological and photodegradation kinetics of polylactide and effect on crystallization rates. *Polym. Degrad. Stab.* **2013**, *98*, 771−784.
(51) Androsch, R.; Schick, C.; Lorenzo, M. L. D. Melting of Conformationally Disordered Crystals (α'-Phase) of Poly(l-lactic acid). *Macromol. Chem. Phys.* **2014**, *215*, 1134−1139.
(52) Kawai, T.; Rahman, N.; Matsuba, G.; Nishida, K.; Kanaya, T.; Nakano, M.; Okamoto, H.; Kawada, J.; Usuki, A.; Honma, N.; Nakajima, K.; Matsuda, M. Crystallization and Melting Behavior of Poly (l-lactic Acid). *Macromolecules* **2007**, *40*, 9463−9469.
(53) Cavallo, D.; Gardella, L.; Soda, O.; Sparnacci, K.; Monticelli, O. Fully bio-renewable multiblocks copolymers of poly(lactide) and commercial fatty acid-based polyesters polyols: Synthesis and characterization. *Eur. Polym. J.* **2016**, *81*, 247−256.
(54) Tseng, F. P.; Lin, J. J.; Tseng, C. R.; Chang, F. C. Poly(oxypropylene)-amide grafted polypropylene as novel compatibilizer for PP and PA6 blends. *Polymer* **2001**, *42*, 713−725.
(55) Lin, Y.; Zhang, K.-Y.; Dong, Z.-M.; Dong, L.-S.; Li, Y.-S. Study of Hydrogen-Bonded Blend of Polylactide with Biodegradable Hyperbranched Poly(ester amide). *Macromolecules* **2007**, *40*, 6257−6267.

https://dx.doi.org/10.1021/acsomega.0c02765
ACS Omega 2020, 5, 26421−26430